DOI: 10.15199/17.2023.5.2

Optimisation of the operating parameters of the natural gas compressor station

???

Andrzej J. Osiadacz, Maciej Chaczykowski*

Keywords: *Compressor station, Optimisation of operating parameters, Compressor fuel cost minimisation, Nonlinear programming*

Abstract
The paper presents an algorithm of automatic search for the optimal values of the operating parameters of the natural gas compressor station. It has been assumed that natural gas can be supplied with two types of compressors: centrifugal compressors and motor-compressors. The nonlinear programming problem with continuous and discrete variables was solved to evaluate the number of simultaneously operating compressors and their operating parameters. The total fuel consumption in each time interval is minimized subject to the constraints imposed.

Słowa kluczowe: *Stacja przetłoczna, Optymalizacja parametrów pracy, Minimalizacja kosztów gazu paliwowego, Programowanie nieliniowe*

Streszczenie
W artykule przedstawiono algorytm automatycznego poszukiwania optymalnych wartości parametrów pracy tłoczni gazu ziemnego. Założono, że gaz ziemny może być dostarczany za pomocą dwóch rodzajów sprężarek: odśrodkowych oraz tłokowych. Rozwiązano problem programowania nieliniowego ze zmiennymi ciągłymi i dyskretnymi w celu optymalizacji liczby jednocześnie pracujących sprężarek i ich parametrów. Minimalizowano całkowite zużycie paliwa w każdym przedziale czasowym z uwzględnieniem nałożonych ograniczeń.

Introduction and background

Natural gas is usually transported by pipeline networks which serve as the most cost effective transportation means. Transmission systems usually have a linear topology corresponding to a linear arrangement of compressor stations. The fuel consumption of compressors is responsible for a large fraction of the costs of gas network operation. Luongo et al. (1989) reported that AGA estimates the operating cost of running the compressor stations to vary between 25% and 50% of the total company's operating budget, therefore minimizing fuel usage is a major objective in the control of gas transmission costs.

This work is concerned with the optimization of a single compressor station operated under transient conditions. More specifically, we consider variable boundary conditions, i.e. unsteady inlet and outlet pressures together with a variable flowrate through the compressor, and search for the optimal values of the operating parameters that minimize the running costs of the compressor station.

An overview of different optimization techniques used for managing the gas transport in pipeline networks can be found in a review paper by Ríos-Mercado and Borraz-Sánchez (2015). Examples of the optimization problems under transient conditions include line-packing problem (Krishnaswami et al., 2004) and compressor station fuel cost minimization problems. The later are based upon hierarchical control and decomposition or mathematical programming approaches. The studies on hierarchical control include those by Larson and Wismer (1971), Osiadacz and Bell (1986), Osiadacz (1994), Osiadacz and Swierczewski (1994) and Osiadacz (1998), while mathematical programming approaches formulate and solve nonlinear programming problems (Ehrhardt and Steinbach, 2005; Steinbach, 2007), mixed integer linear programming problems based on piecewise linearization (Moritz, 2007; Mahlke et al., 2010), or combination of the linear and nonlinear formulations (Domschke et al., 2011).

This paper builds on (Osiadacz and Bell, 1981) and (Osiadacz, 1980) works, where local optimization procedure of the compressor station and an algorithm of automatic search for the optimal values of the operating parameters were proposed. The optimization procedure minimizes the compressor driver's fuel consumption, while the algorithm automatically searches the number of simultaneously operating compressors and their capacity distribution.

In particular, the work here is to model the dynamics of the pipeline sections adjacent to the compressor station (in a linear network configuration) by means of hyperbolic PDE system representing mass, momentum and energy conservation laws instead of parabolic PDE describing isothermal flow conditions. The conservation equations are coupled with the equation of state for a real gas, and the modeling considers 24 to 48 h time frame to asses the daily variations in gas demand.

The decision variables of the centrifugal compressors are the rotational speeds, while the decision variables of motor-compressors are the rotational speeds and the operating modes (number of

* **Andrzej J. Osiadacz, Maciej Chaczykowski,** Warsaw University of Technology, 20 Nowowiejska St, 00-653 Warsaw, Poland

clearance pockets which are opened to or closed from the cylinder space). A set of constraints is developed based on flow model equations and operating conditions of the compressors. Due to the nonlinearity of the constraints and the objective function, the developed model is a nonlinear programming problem.

Governing equations

In the following we describe the cost function of the transient optimization problem, its physical and technical restrictions, followed by appropriate space and time discretizations by an implicit method. Finally, a brief description of the method used to determine optimal values of the decision variables is provided.

Centrifugal compressor equations

The compressor equations describe the thermodynamic properties of gas during the flow across the compressor and allow to determine the compressor performance. The power necessary to drive the compressor is

$$P = \frac{\rho_S Q_S H_{is}}{\eta_{is}\eta_{mech}} \tag{1}$$

The isentropic head developed by the compressor is the amount of energy supplied to the gas per unit mass of the gas

$$H_{is} = zRT\frac{k}{k-1}\left[\varepsilon^{(k-1)/k} - 1\right] \tag{2}$$

The performance of centrifugal compressors can be characterized in terms of inlet volumetric flow rate $Q = Q(p, T)$, speed ω, isentropic head and isentropic efficiency. The relationships between these quantities are usually represented by performance maps in the form of plots of H and η_{is} at variety of speeds as shown in Fig. 1 and Fig. 2. Using three normalized parameters, namely H/ω^2, Q/ω^2, η_{is} and cubic polynomial functions with constant parameters fitted by least square method, the performance maps are approximated by (Odom, 1991)

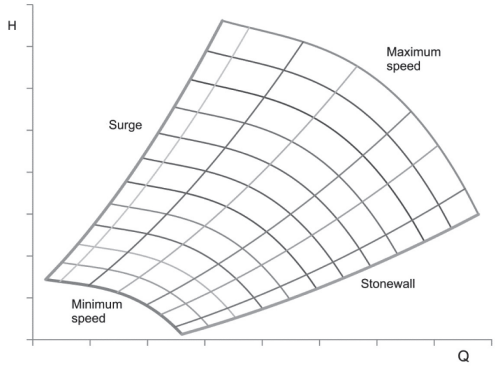

Figure 1 – Centrifugal compressor map H as a function of Q and ω.
Rysunek 1 – Charakterystyka sprężarki odśrodkowej H w funkcji Q i ω.

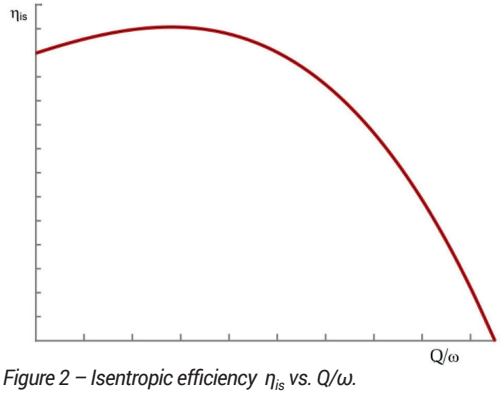

Figure 2 – Isentropic efficiency η_{is} vs. Q/ω.
Rysunek – Izentropowa sprawność we współrzędnych η_{is} i Q/ω.

$$\frac{H_{is}}{\omega^2} = a_1 + a_2\left(\frac{Q}{\omega}\right) + a_3\left(\frac{Q}{\omega}\right)^2 + a_4\left(\frac{Q}{\omega}\right)^3 \tag{3}$$

$$\eta_{is} = a_5 + a_6\left(\frac{Q}{\omega}\right) + a_7\left(\frac{Q}{\omega}\right)^2 + a_8\left(\frac{Q}{\omega}\right)^3 \tag{4}$$

Equations (3) and (4) characterize the specific centrifugal compressor map and are valid in the operational range of the compressor, limited by the maximum and minimum allowable speed, as well as surge and stone limits as shown in Figure 1.

The rotational speed limits can be written as

$$\omega_{\min} \le \omega \le \omega_{\max} \tag{5}$$

The surge and the stonewall limits are determined using the following relation

$$\frac{Q_L}{\omega_{\min}} \le \omega \le \frac{Q_U}{\omega_{\max}} \tag{6}$$

The fuel consumption for the compressor driver is obtained by

$$Q_{S\,fuel} = \frac{P}{LHV\,\eta_{dr}} \tag{7}$$

while the gas discharge temperature is approximated by

$$T_d = T_s + \frac{T}{\eta_{is}}\left[\varepsilon^{(k-1)/k} - 1\right] \tag{8}$$

The fuel is taken directly from the gas flow, therefore the mass balance for the suction and discharge of the compressor station is

$$Q_{Ss} - Q_{Sfuel} = Q_{Sd} \tag{9}$$

Reciprocating compressor equations

The effective power of motocompressor may be expressed in terms of polytropic head Hp

$$P = \frac{\rho_S Q_S H_p}{\eta_{mech}} \tag{10}$$

where

$$H_p = zRT\frac{m_1}{m_1 - 1}\left[\varepsilon^{(m_1-1)/m_1} - 1\right] \tag{11}$$

The characteristics of motocompressor are given by the following formulae

$$P = P(Q_S) \tag{12}$$

$$Q_S = Q_S(\omega, C) \tag{13}$$

$$Q = \mu\left[1 - C\left(\varepsilon^{1/m_2} - 1\right)\right]V_S\omega s \tag{14}$$

$$Q_S = \frac{pQT_S}{ZTp_S} \tag{15}$$

The operational characteristic of a motorcompressor is defined explicitly by the load characteristic which presents the relation bitween the unit fuel consumption and the torque or the effective power at constant speed (Osiadacz, 1980)

$$\frac{Q_{S\,fuel}}{P} = a_9\omega^4 + a_{10}\omega^3 + a_{11}\omega^2 + a_{12}\omega + a_{13} \tag{16}$$

where the coefficients a_9, a_{10}, a_{11}, a_{12}, a_{13} are functions of p, C and ε. We assume that each compressor is a double-acting two-cylinder machine. Both ends of the cylinder are fitted with clearance pockets, each opened to the cylinder space or closed from the cylinder space by a valve controlled from the operator's control panel. The analysis of the moto-compressor load characteristics

shows that the higher te speed the lower is the specific fuel consumption (Osiadacz and Bell, 1981). The detailed description of the motocompressor operational characteristic is given in the study by Osiadacz (1980).

PIPE EQUATIONS

The non-isothermal flow of gas in pipe segments adjacent to the compressor station is governed by the time-dependent continuity, motion, and energy equations for one-dimensional pipe flow and an equation of state for real gas.

Since pressure and volumetric flow rate at normal conditions (or mass flow rate) are of primary interest for pipeline operators, the continuity, momentum, and energy equations that include the effects of wall friction and heat transfer should be written in terms of pressure and volumetric flow rate

$$\frac{\partial p}{\partial t}-\left[\frac{1}{T}+\frac{1}{z}\left(\frac{\partial z}{\partial T}\right)_p\right]\left[\frac{1}{p}-\frac{1}{z}\left(\frac{\partial z}{\partial p}\right)_T\right]^{-1}\frac{\partial T}{\partial t} +\frac{\rho_S zRT}{pA}\left[\frac{1}{p}-\frac{1}{z}\left(\frac{\partial z}{\partial p}\right)_T\right]^{-1}\frac{\partial Q_S}{\partial x}=0 \tag{17}$$

$$\frac{\partial Q_S}{\partial t}-\frac{\rho_S Q_S zRT}{pA}\left\{-2\frac{\partial Q_S}{\partial x}+Q_S\left[\frac{1}{p}-\frac{1}{z}\left(\frac{\partial z}{\partial p}\right)_T\right]\frac{\partial p}{\partial x} -Q_S\left[\frac{1}{T}+\frac{1}{z}\left(\frac{\partial z}{\partial T}\right)_p\right]\frac{\partial T}{\partial x}\right\}+\frac{A}{\rho_S}\frac{\partial p}{\partial x} +\frac{fzRT\rho_S Q_S|Q_S|}{2DAp}+\frac{p}{zRT\rho_S}g\sin\alpha=0 \tag{18}$$

$$\frac{\partial T}{\partial t}+\frac{\rho_S Q_S zRT}{pA}\frac{\partial T}{\partial x} +\frac{RT}{c_v}\frac{\rho_S Q_S zRT}{pA}zT\left[\frac{1}{T}+\frac{1}{z}\left(\frac{\partial z}{\partial T}\right)_\rho\right] \times\left\{\frac{1}{Q_S}\frac{\partial Q_S}{\partial x}-\left[\frac{1}{p}-\frac{1}{z}\left(\frac{\partial z}{\partial p}\right)_T\right]\frac{\partial p}{\partial x} +\left[\frac{1}{T}+\frac{1}{z}\left(\frac{\partial z}{\partial T}\right)_p\right]\frac{\partial T}{\partial x}\right\} -\frac{f}{2c_v D}\left(\frac{zRT\rho_S|Q_S|}{Ap}\right)^3-\frac{q}{c_v}=0 \tag{19}$$

$$p/\rho = zRT \tag{20}$$

where x and t are the local coordinate along the pipe and time, respectively, while p, Q_S, and T are, respectively, the gas pressure, volumetric flow rate at standard conditions, and gas temperature. The last two terms on the left hand side of Eq. (18) represent, respectively, the effect of viscous friction at the pipe wall, where f is the Darcy friction factor and D is the pipeline diameter, and the net body force acting on the gas, where g is the acceleration of gravity and α is the angle between the horizon and the direction x (pipe inclination). The heat transfer term q in Eq. (19) represents the amount of heat exchanged between unit mass of gas and the surroundings per unit time, while A is the pipe cross section, c_v is the heat capacity of the gas at constant volume, and ρ_S is the gas density at standard conditions. The compressibility factor z describes the deviation (of multiplicative type) of the real gas volume from the ideal gas volume at given p-T conditions. In this study it was calculated according to the GERG88 formula.

Numerical scheme

The systems of partial differential equations represented by Eqs. (1)-(3) are solved by the implicit finite difference method (Kiuchi, 1994). Finite difference methods have commonly been used to model the flow of natural gas through pipeline systems with implicit methods being preferred to explicit, as these are stable for any choice of time and spatial discretization step.

The pipelines are divided into N sections, i.e. a uniform one-dimensional mesh consisting of N+1 points: x_1, … x_{N+1} is used (Fig. 3). The temporal derivatives of the dependent variables $Y = (p, Q_S, T)$ for the jth pipe section (between mesh points i and i+1) are approximated by

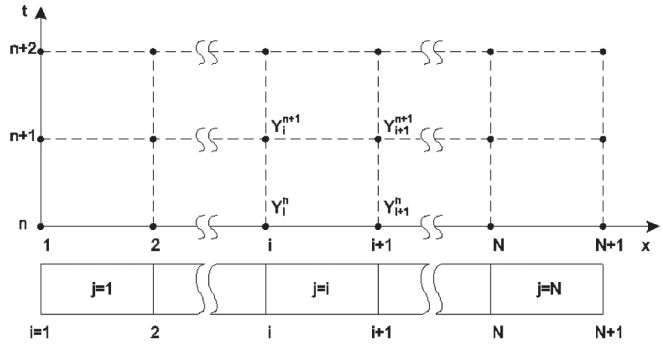

Figure 3 – Discretization scheme and computational stencil of the finite difference method.
Rysunek 3 – Schemat dyskretyzacji i schemat obliczeniowy metody różnic skończonych.

$$\frac{\partial Y(j,t_{n+1})}{\partial t}=\frac{Y_{i+1}^{n+1}+Y_i^{n+1}-Y_{i+1}^n-Y_i^n}{2\Delta t}+O(\Delta x^2),\ j=1,N \tag{21}$$

The spatial derivatives are approximated by

$$\frac{\partial Y(j,t_{n+1})}{\partial x}=\frac{1}{\Delta x}\left(-Y_i^{n+1}+Y_{i+1}^{n+1}\right) \tag{22}$$

and the individual terms by

$$Y(j,t_{n+1})=\frac{Y_{i+1}^{n+1}+Y_i^{n+1}}{2} \tag{23}$$

The guaranteed stability of the fully implicit method for large time step is very useful for simulating long term transients in natural gas pipelines. The short computation time makes fully implicit methods very attractive for gas pipeline applications.

Formulation of the optimization problem

We wish to operate the compressrs in the station in such a way that total fuel consumption is minimized while satisfying the operational limitations. The control variables on subinterval $(t\text{-}1,t)$ are piecewise constant. In our formulation, the control variables are chosen to be the number of units in the compressor station K and their operation speeds ω. In the case of the reciprocating compressors additional decision variable C corresponds with the number of clearance pockets open to-/closed from-cylinder space.

The states at time t consist of the nodal pressures $p(j,t)$ and flows $Q_s(j,t)$, and further states in centrifugal compressors consist of $s_t = s(K,\omega)$ and reciprocating compressors $s_t = s(K,\omega,C)$, respectively. The optimization of the compressor station is formulated as a mixed integer nonlinear programming problem.

Figure 4 shows the control block diagram for the pipeline transportation system considered in this study. The optimization algorithm, based on predicted gas demand Q(t), finds a value of vector x, defined by

$$\boldsymbol{x} = \begin{bmatrix} \omega_1 \\ \omega_2 \\ \vdots \\ \omega_K \end{bmatrix} \tag{24}$$

for a given value of vector y

$$\boldsymbol{y} = \begin{bmatrix} Q_S \\ p_d \\ p_s \end{bmatrix} \tag{25}$$

which together with the assumed value of vector z

$$\boldsymbol{z} = \begin{bmatrix} Q_{S1}/\ \omega_1 \\ Q_{S2}/\ \omega_2 \\ \vdots \\ Q_{SK}/\ \omega_K \end{bmatrix} \tag{26}$$

minimizes the value of fuel consumption at a defined time interval. The components of the vector Z take only defined values determined by the feasible values of factor *C*.

There are the following constraints resulting from the speed limits and mass balance of the compressors, respectively

$$g_{i,k}\left(\mathbf{x}^{\mathrm{T}}\mathbf{e}_k\right) \le 0,\ i = 1,2 \tag{27}$$

$$h(\mathbf{x}) = \mathbf{x}^{\mathrm{T}}\mathbf{z} - Q_S = 0 \tag{28}$$

The set of equations (27) accounts for the rotational speed limits, i.e.

$$\left.\begin{aligned} g_1\left(\mathbf{x}^{\mathrm{T}}\mathbf{e}_k\right) &= \omega_{\min} - \mathbf{x}^{\mathrm{T}}\mathbf{e}_k \le 0 \\ g_2\left(\mathbf{x}^{\mathrm{T}}\mathbf{e}_k\right) &= \mathbf{x}^{\mathrm{T}}\mathbf{e}_k - \omega_{\max} \le 0 \end{aligned}\right\}\ k = 1,2\mathrm{K}\ K \tag{29}$$

A control algorithm determines the number *K* of machines necessary for the task realization by computing the integer part of $(QS/QSk(\omega_{max}) + 1)$. In the next step, a matrix $\mathrm{W} = [w_{i,k}]_{I,K}$ of feasible combinations values of factors *C* for the *K* machines is determined. As an example, for $K = 3$, given that there are three operating modes available for each machine, which correspond to 1) all pockets closed $C = C_1$, 2) all pockets opened $C = C_2$, and 3) each cylinder has one pocket opened $C = C_3$, the matrix W will be a 3 column matrix with 9 rows as follows

$$\mathbf{W} = \begin{bmatrix} C_1 & C_1 & C_1 \\ C_1 & C_1 & C_2 \\ C_1 & C_1 & C_3 \\ C_1 & C_2 & C_2 \\ C_1 & C_2 & C_3 \\ C_1 & C_3 & C_3 \\ C_2 & C_2 & C_2 \\ C_2 & C_2 & C_3 \\ C_3 & C_3 & C_3 \end{bmatrix} \tag{30}$$

Next, the algorithm determines the initial distribution of the capacity between the individual machines Q_{Sk}, $k = 1, 2,..., K$ given the values of suction pressure ps, discharge pressure pd and total flow rate through the compressor station Q_S. Finally, the speeds ω_k, $k = 1, 2,..., K$ are determined over the set of feasible points that minimize the fuel consumption for the individual rows of the matrix W. The computation results in a feasible sequence of values of the objective function from among which the minimum value is selected

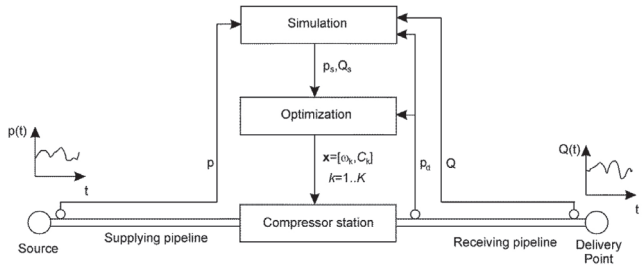

Figure 4 – Control block diagram for the pipeline transportation system considered in this study.

Rysunek 4 – Schemat blokowy sterowania dla systemu transportu gazu analizowanego w tej pracy.

$$\min\left\{\sum_{k=1}^{K} f_{i,k}\right\} i = 1,\mathrm{K}\ I \tag{31}$$

The values K_k, ω_k, and C_k that satisfy the condition (31) are the solution of the optimization problem.

In the previous studies on nonlinear optimization in gas networks (Krishnaswami et al., 2004; Ehrhard and Steibach, 2005) the time frame was divided equidistantly to yield a time grid with the constant length of subintervals Δt. In this study the time grid is related to the time rate of change of the elements of vector y(*t*)

$$\mathbf{y}(t) = \begin{bmatrix} Q_S(t) \\ p_d(t) \\ p_s(t) \end{bmatrix} \tag{32}$$

Since the control variables on every time subinterval are piecewise constant, the vector y(*t*) is approximated by a staircase function

$$\tilde{\boldsymbol{y}}(t) = \begin{cases} y(1) \text{ for } t_0 \le t < t_1 \\ y(2) \text{ for } t_1 \le t < t_2 \\ \vdots \\ y(N) \text{ for } t_{N-1} \le t < t_N \end{cases} \tag{33}$$

where t_N is the observation time. The length of time intervals is assigned for the condition

$$\sup_t |\boldsymbol{y}(t) - \tilde{\boldsymbol{y}}(t)| \le \boldsymbol{\delta} \tag{34}$$

where δ is suitably chosen vector given by $[\Delta Q_s, \Delta\rho_d, \Delta\rho_s]^{\mathrm{T}}$.

Solution of the optimization problem

Conjugate gradient method was used to determine optimal values of ω_k. The objective function was

$$P(\mathbf{x}, r_1^m, r_2^m) = f(x) + r_1^m F_1(x) + r_2^m F_2(x) \tag{35}$$

where the penalty functions were expressed as

$$F_1(\mathbf{x}) = \left(\max\left(0, |h(\mathbf{x})|\right)\right)^2 \tag{36}$$

$$F_2(\mathbf{x}) = \sum_{i=1}^{2}\sum_{k=1}^{K}\left(\max\left(0, \left|g_i(\mathbf{x}^{\mathrm{T}}e_k)\right|\right)\right)^2 \tag{37}$$

Values of the multiplier were determined from relations $r_1^{\mathrm{m}} = a_1 b_1^{\mathrm{m}}$, $r_2^{\mathrm{m}} = a_2 b_2^{\mathrm{m}}$ where *m* is the number of iterations.

The necessary condition that the function $P(\mathrm{x}, r_1^{\mathrm{m}}, r_2^{\mathrm{m}})$ has a stationary value is

$$\nabla_{\mathrm{x}} P(\mathbf{x}, r_1^m, r_2^m) = \nabla_{\mathrm{x}} f(\mathbf{x}) + r_1^m \nabla_{\mathrm{x}} F_1(\mathbf{x}) + r_2^m \nabla_{\mathrm{x}} F_2(\mathbf{x}) = \mathbf{0} \tag{38}$$

where the elements of the respective vectors are

$$\nabla_{\mathbf{x}} f(\mathbf{x}) = \begin{bmatrix} \partial f_1 / \partial \omega_1 \\ \mathrm{M} \\ \partial f_K / \partial \omega_K \end{bmatrix}$$

$$\nabla_{\mathbf{x}} F_1(\mathbf{x}) = 2\left(\sum_{k=1}^{K} B_k \omega_k - Q_S\right) \begin{bmatrix} B_1 \\ \mathrm{M} \\ B_K \end{bmatrix}$$

$$\nabla_{\mathbf{x}} F_2(\mathbf{x}) = 2 \begin{bmatrix} -\max\left(0, \left|g_1(\mathbf{x}^{\mathrm{T}} e_1)\right|\right) + \max\left(0, \left|g_2(\mathbf{x}^{\mathrm{T}} e_1)\right|\right) \\ \mathrm{M} \\ -\max\left(0, \left|g_1(\mathbf{x}^{\mathrm{T}} e_K)\right|\right) + \max\left(0, \left|g_2(\mathbf{x}^{\mathrm{T}} e_K)\right|\right) \end{bmatrix}$$

while $B_k = Q_{Sk} / \omega_k$. Initial values were assumed as $a_1 = 1.0$, $b_1 = 2.5$, $a_2 = 5.0$, $b_2 = 7.8$.

Results and discussion

The efficiency of the optimal control algorithm has been checked by using telemetry data from two different scale gas transmission systems with compressor stations incorporating gas turbine driven centrifugal compressors and internal combustion engine driven reciprocating compressors, respectively. The stations with reciprocating compressors are equipped with water-cooled aftercoolers which results in an isothermal flow conditions in the receiving pipelines, while the stations with centrifugal compressors are equipped with aerial aftercoolers causing significant temperature difference between the discharged gas and the pipeline surroundings. The tests were made for various gas supply and consumer demand conditions. Selected results of this tests are present in this study.

The boundary conditions (the values of pressure at $x = 0$ on the supplying pipe and the flow rate at $x = L$ on the receiving pipe) for centrifugal compressors operating scenario are presented in Figures 5-7, while the boundary conditions for reciprocating compressors operating scernario are shown in Fig. 11-13. The results of the calculations of flow conditions in the respective operating scernarios are shown in Figures 8-10 and 14-16. The input data regarding the geometry of the pipelines are presented in Table 1. The

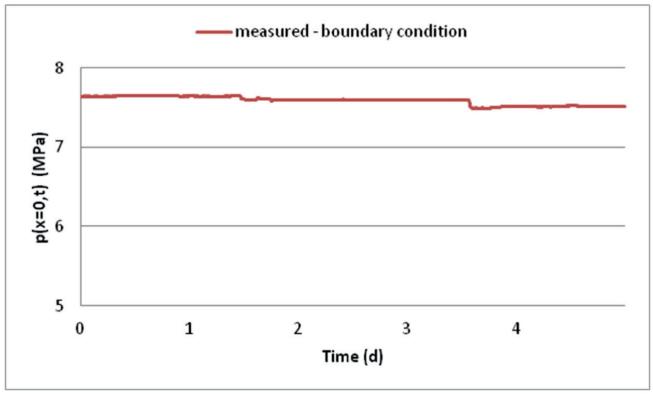

Figure 5 – Pressure at x = 0 on the supplying pipe of centrifugal compressors.
Rysunek 5 – Ciśnienie w x = 0 na przewodzie zasilającym sprężarki odśrodkowe.

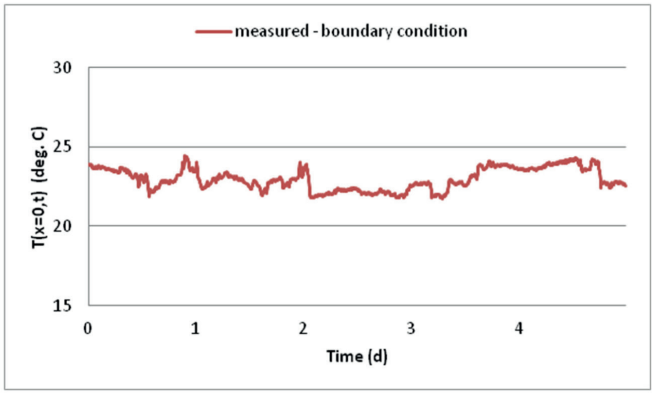

Figure 6 – Temperature at x = 0 on the supplying pipe of centrifugal compressors.
Rysunek 6 – Temperatura w x = 0 na przewodzie zasilającym sprężarki odśrodkowe.

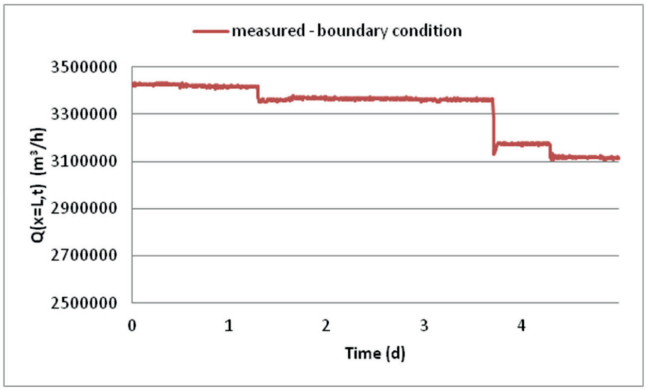

Figure 7 – Flow rate at x = L on the receiving pipe of centrifugal compressors,
Rysunek 7 – Natężenie przepływu w punkcie x = L na przewodzie odbiorczym sprężarek odśrodkowych

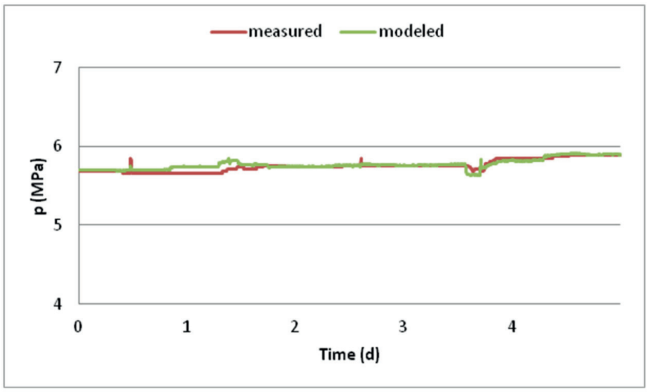

Figure 8 – Example of model validation: pressure at x = L on the supplying pipe of centrifugal compressors,
Rysunek 8 – Przykład walidacji modelu: ciśnienie w punkcie x = L na przewodzie zasilającym sprężarki odśrodkowe

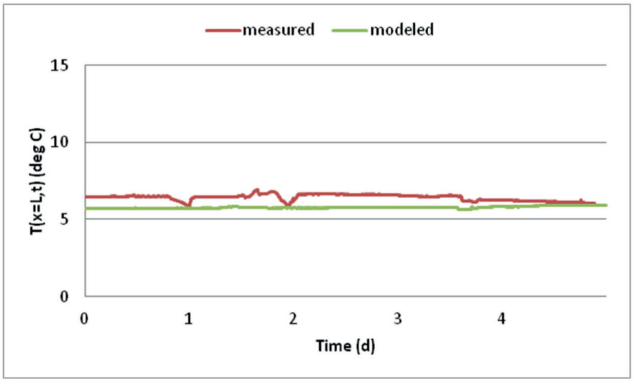

Figure 9 – Example of model validation: temperature at x = L on the supplying pipe of centrifugal compressors,
Rysunek 9 – Przykład walidacji modelu: temperatura w punkcie x = L na przewodzie zasilającym sprężarki odśrodkowe

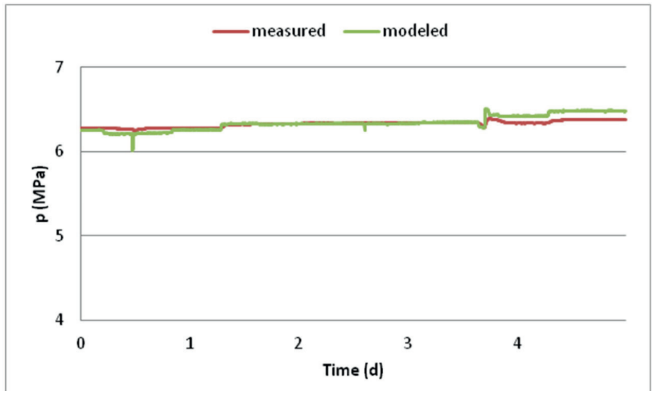

Figure 10 – Example of model validation: pressure at x = L on the receiving pipe of centrifugal compressors,

Rysunek 10 – Przykład walidacji modelu: ciśnienie w punkcie x = L na przewodzie odbiorczym sprężarek odśrodkowych

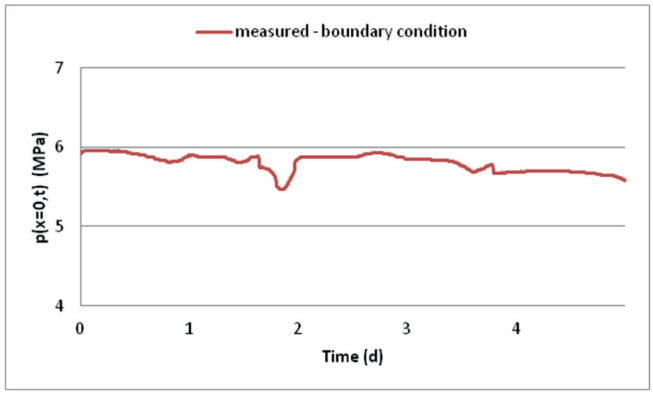

Figure 11 – Pressure at x = 0 on the supplying pipe of reciprocating compressors.

Rysunek 11 – Ciśnienie przy x = 0 na przewodzie zasilającym sprężarki tłokowe.

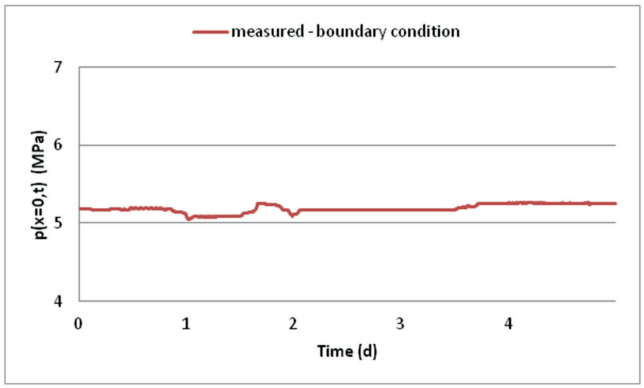

Figure 12 – Pressure at x = 0 on the receiving pipe of reciprocating compressors.

Rysunek 12 – Ciśnienie przy x = 0 na przewodzie odbiorczym sprężarek tłokowych.

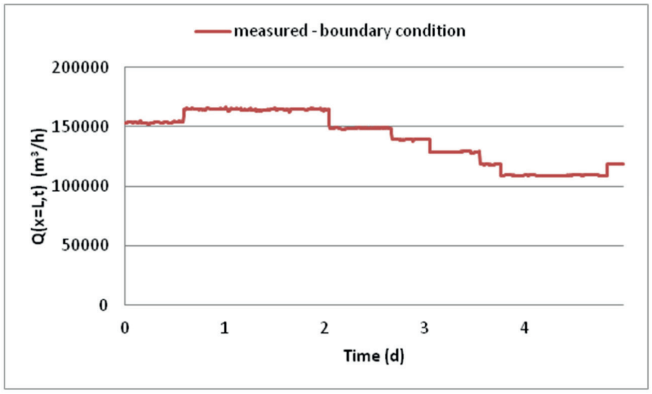

Figure 13 – Flow rate at x = L on the receiving pipe of reciprocating compressors.

Rysunek 13 – Natężenie przepływu przy x = L na przewodzie odbiorczym sprężarek tłokowych.

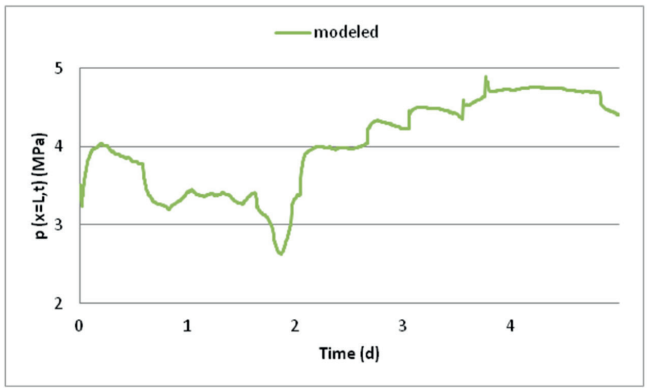

Figure 14 – Pressure at x = L on the supplying pipe of reciprocating compressors.

Rysunek 14 – Ciśnienie w punkcie x = L na przewodzie zasilającym sprężarki tłokowe.

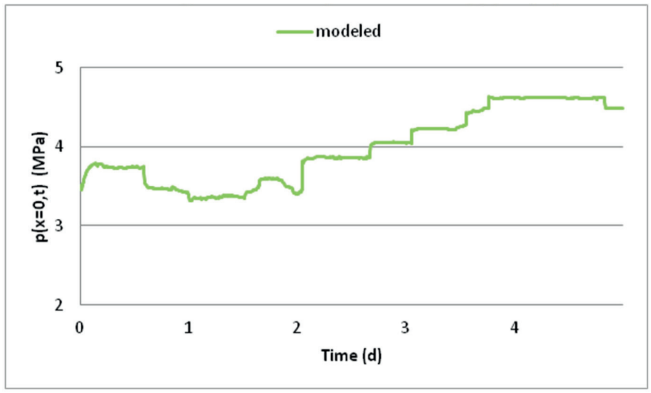

Figure 15 – Pressure at x = L on the receiving pipe of reciprocating compressors.

Rysunek 15 – Ciśnienie w punkcie x = L na przewodzie odbiorczym sprężarek tłokowych.

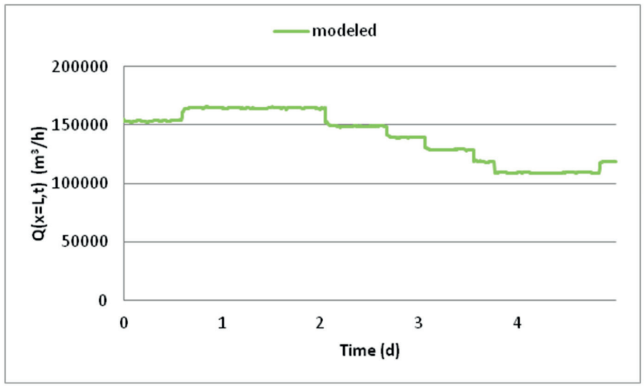

Figure 16 – Flowrate at x = L on the supplying pipe of reciprocating compressors.

Rysunek 16 – Strumień przepływu przy x = L na przewodzie zasilającym sprężarki tłokowe.

intervention frequency of the optimizing algorithm depends on the assumed sensitivity threshold value of the vector δ. The following magnitudes of the elements of vector δ in Eq. (34) were assumed in the example with centrifugal compressors: $|\Delta p_d|=|\Delta p_s|=0.05$ MPa (7.25 psi) and $|\Delta Q_S|=100{,}000$ m^3/h (3.5 MMCFH). The respective values in the example with reciprocating compressors were: 0,1 MPa and 10,000 m^3/h. Sample results of the algorithm controlling a gas compressor station with centrifugal compressors rated 25.4 MW with maximum compresson ratio of 1.4 are shown in Table 2, while the respective results obtained for the algorithm solving motor-compressors with characteristics given by $P = 882$ kW and $\varepsilon_{max} = 1.9$ are presented in Table 3.

Table 1. Input data concerning pipeline systems.
Tabela 1. Dane wejściowe dotyczące systemów przesyłowych.

	Supplying pipeline		Receiving pipeline	
Compressor type (scenario)	Centrifugal	Reciprocating	Centrifugal	Reciprocating
Diameter, mm	1400	500	1400	500
Length (km)	177	174	139	110
Pipe roughness (mm)	0.005	0.1	0.005	0.1

Table 2. Results of optimization (centrifugal compressors).
Tabela 2. Wyniki optymalizacji (sprężarki odśrodkowe).

Interval time	Total capacity Q_S, m^3/h	Capacity distribution Q_{Sk} (m^3/h)	Suction pressure p_s, MPa	Discharge pressure p_d, MPa (PSI)	Number of compressors operating simultaneously K	Rotational speed ω_k (r.p.m.)	Effective power distribution P_k (MW)
0	3 428 250	1 142 750 1 142 750 1 142 750	5.694	7.633	3	4892 4892 4892	13.83 13.83 13.83
1	3 411 136	1 705 568 1 705 568 1 705 568	5.740	7.632	2	7178 7178	20.07 20.07
2	3 366 791	1 683 395 1 683 395 1 683 395	5.744	7.560	2	7002 7002	19.08 19.08
3	3 169 696	1 584 848 1 584 848 1 584 848	5.814	7.511	2	6394 6394	16.78 16.78
4	3 123 696	1 561 848 1 561 848 1 561 848	5.894	7.584	2	6134 6134	15.64 15.64

Table 3. Results of optimization (reciprocating compressors).
Tabela 3. Wyniki optymalizacji (sprężarki tłokowe).

Interval time	Total capacity Q_S, m^3/h	Capacity distribution Q_{Sk} (m^3/h)	Suction pressure p_s, MPa	Discharge pressure p_d, MPa	Number of compressors operating simultaneously K	Ratio of clearence volume to swept volume C_k	Rotational speed ω_k (r.p.m.)	Effective power distribution P_k (MW)
0	152 991	50 997 50 997 50 997	3.453	5.179	3	**2** **2** **2**	291 291 291	694 694 694
1	164 693	51 740 56 476 56 476	3.313	5.081	3	**2** **3** **3**	320 320 320	746 815 815
2	149 314	49 771 49 771 49 771	3.403	5.172	3	**2** **2** **2**	295 295 295	701 701 701
3	130 774	65 387 65 387	4.046	5.257	2	**2** **2**	262 262	565 565
4	104 297	104 297	4.622	5.252	1	**1**	319	431

Conclusions

An optimization procedure has been presented which minimizes the compressor driver's fuel consumption.This algorithm takes into consideration information concerning the dynamics of the pipelines adjacent to the compressor station by incorporating the transient non isothermal gas flow model. The hydraulic model allows for the accurate prediction of the working paramaters in the pipelines. The results presented in this paper suggest that the proposed procedure is attractive from a computational point of view and can lead to significant reduction in fuel consumption. It can also be easily extended to account for other compressor station operation related costs, such as costs of CO_2 emissions and the costs of start/stop operation of the machines. ■

LITERATURA

[1] Domschke, P., Geißler, B., Kolb, O., Lang, J., Martin, A., Morsi, A. (2011) Combination of nonlinear and linear optimization of transient gas networks. INFORMS Journal on Computing, 23(4), 605–617.

[2] Ehrhardt, K., Steinbach, M.C. (2005) Nonlinear optimization in gas networks. In: Bock, H.G. (Ed.) Modeling, simulation and optimization of complex processes. Springer, Berlin-Heidelberg, pp. 139–148.

[3] Krishnaswami, P., Chapman, K.S., Abbaspour, M. (2004) Compressor station optimization for linepack maintenance. In: Proceedings of the 36th PSIG Annual Meeting, Palm Springs, PSIG 0410.

[4] Larson, R.E., Wismer, D.A. (1971) Hierarchical control of transient flow in natural gas pipeline networks. In: Proceedings of the IFAC Symposium on Distributed Parameter Systems, Banff, Alberta, Canada.

[5] Luongo, C.A., Gilmour, B.J., Schroeder, D.W. (1989) Optimization in Natural Gas Transmission Networks: A Tool to Improve Operational Efficiency. Proceedings of the 3rd SIAM Conference on Optimization, pp. 110–117.

[6] Mahlke, D., Martin, A., Moritz, S. (2010) A mixed integer approach for time-dependent gas network optimization. Optimization Methods & Software, 25(4), 625–644.

[7] Moritz, S. (2007) A mixed integer approach for the transient case of gas network optimization. PhD thesis, Darmstadt University of Technology.

[8] Odom, F.M., Muster, G.L. (2009) Tutorial on Modeling of Gas Turbine Driven Centrifugal Compressors. In: Proceedings of the 40th PSIG Annual Meeting, Galveston. PSIG-09A4.

[9] Osiadacz, A.J. (1980) Nonlinear programming applied to the optimum control of a gas compressor station. International Journal for Numerical Methods in Engineering 15(9), 1287–1301.

[10] Osiadacz, A.J. (1994) Dynamic optimization of high pressure gas networks using hierarchical systems theory. In: Proceedings of the 26th PSIG Annual Meeting, San Diego. PSIG-9408.

[11] Osiadacz, A.J. (1998) Hierarchical control of transient flow in natural gas pipeline systems. International Transactions on Operational Research 5(4):285–302.

[12] Osiadacz, A.J., Bell, D.J. (1986) A simplified algorithm for optimization of large-scale gas networks. Optimal Control Applications and Methods 7(1):95–104.

[13] Osiadacz, A.J., Swierczewski, S. (1994) Optimal control of gas transportation systems. In: Proceedings of the 3rd IEEE Conference on Control Applications, Glasgow, UK, pp. 795–796.

[14] Ríos-Mercado, R.Z., Borraz-Sánchez, C. (2015) Optimization problems in natural gas transportation systems: A state-of-the-art review. Applied Energy, 147, 536–555.

[15] Steinbach, M.C. (2007). On PDE solution in transient optimization of gas networks. Journal of Computational and Applied Mathematics, 203(2), 345–361.

[16] Kiuchi, T. (1994) An implicit method for transient gas flows in pipe networks. International Journal of Heat and Fluid Flow 15:378–383.